Proceedings of the ASME 2015 International Design Engineering Technical Conferences & Computers and Information in Engineering Conference
IDETC/CIE 2015
August 2-5, 2015, Boston, Massachusetts, USA

DETC2015-47703

MODELING AND DYNAMIC PARAMETER IDENTIFICATION OF THE SCHUNK POWERBALL ROBOTIC ARM

Amirhossein H. Memar
Department of Mechanical and Aerospace Engineering, University at Buffalo SUNY
Buffalo, New York, US
ahajiagh@buffalo.edu

Ehsan T Esfahani
Department of Mechanical and Aerospace Engineering, University at Buffalo SUNY
Buffalo, New York, US
ehsanesf@buffalo.edu

ABSTRACT

This paper presents the modeling and dynamic parameter identification of the 6-DoF SCHUNK Powerball LWA 4P robotic arm. Precise positioning, zero backlash and compact design of the joints which integrate two perpendicular axes, make this robot ideal for service robotics applications and human-robot interaction. Due to the significant effect of the lubricant temperature on the behavior of viscous friction in the harmonic drives, a systematic procedure is developed to overcome this problem. A series of experiments have been conducted to model the friction at each joint, then the procedure of identification has been applied based on an inverse dynamic model and linear least-square techniques. Finally, a verification trajectory is executed by the robot to validate the estimated parameters of the system.

I. INTRODUCTION

The dynamic model of the robot is essential for implementation of advanced model-based control algorithms. The performance of most of these techniques is significantly dependent on the accuracy of the dynamic model to maintain high levels of precision and reliability. On the other hand, small tracking errors along with high-speed motion cannot be achieved using the traditional independent joint controller based on PID controllers. Moreover, implementation of impedance control methods, which is essential during human-robot interaction, are not feasible without having robot dynamic model. Therefore, the accuracy of dynamic parameters of the robot plays an important role in the dexterous manipulation and robot interaction with the environment and humans.

Normally the dynamic models of industrial robots are not available; therefore, an identification procedures should be utilized to identify unknown model parameters. Moreover, direct measurement of these parameters is not feasible always and can cause damages to the system, because this procedure requires dismantling the robot parts and measuring inertial parameters link by link. Another problem with this approach is that some of nonlinear inherent properties at the robot joints such as friction and compliance cannot be measured directly; therefore, a systematic procedure should be used.

The SCHUNK Powerball LWA (Fig. 1) is a lightweight 6-DoF robotic arm consisting of three major compact joints named ERB modules that integrate two perpendicular axes along with their overall electrical control circuits. Precise positioning of the robot actuators, which is afforded by using zero backlash harmonic drives, makes this manipulator ideal for high precision robotic tasks. In addition, the lightweight and compact design of the robot provide the capability of using it in Human-Robot Interaction (HRI) applications.

Figure 1. SCHUNK POWERBALL LWA 4P

Unfortunately, to our knowledge, there is no publication on the identification of the Powerball dynamic model and the manufacturer does not provide any information about it. The purpose of this paper is to present our results for estimating a dynamic model for the Powerball. We believe that it will be valuable for the future studies using this manipulator.

Dynamic parameter identification of robotic manipulators has been widely analyzed. Several methods based on the linearity property of the manipulator dynamic model are proposed [1][2]. In most of these methods, Least Square techniques are utilized to estimate dynamic parameters. Symbolical or numerical ways can be used to reduce and simplify the linear dynamic model and to ensure that the regressor matrix has a full rank [3]. Successful results of implementing this technique on several lightweight industrial manipulators, i.e. Mitsubishi PA-10 [4] or KUKA LWR [5][6], assert the efficiency of this method. In the identification procedure, exciting trajectory has a significant effect on the convergence and accuracy of the identified parameters, thus exciting trajectory should be optimized to prevent inaccurate estimation [7]. For the purpose of exciting trajectory design, several criterion have been proposed in the literature.

In this paper, the dynamic parameter identification of Powerball robotic arm has been performed using the linear dynamic model and the Least Squares estimation. For this purpose, both kinematic and inverse dynamic models of the robot are derived and then transformed into a simplified linear inverse dynamic model that is developed based on kinematic parameters of the robot. A systematic procedure has been proposed to minimize the effect of lubricant temperature in the friction model of harmonic drives, which results in time varying behavior of viscous friction in the robot joints. Friction model at each joint is developed utilizing a continuously differentiable friction model. Finally, the full set of dynamic parameters has been identified through experiments and the accuracy of the identified model is verified through a trajectory that covers most of the robot workspace.

This paper is organized as follows. Section II presents the kinematic, dynamic and nonlinear friction models for the Powerball manipulator. In section III, after providing a brief summary of the experimental setup, the procedure of designing exciting trajectory is presented. Finally, results of the model identification and verification are reported.

II. MODELING

A. Kinematic Model

The SCHUNK Powerball LWA 4P is an anthropomorphic robotic arm with a spherical wrist. Figure 2 illustrates the schematic representation of the kinematic chain of the robot considering vertical mounting. The frame assignment of the entire structure has been done using the well-known Denavit-Hartenberg (D-H) method. The standard D-H parameters for the robot structure are specified in Tab. 1.

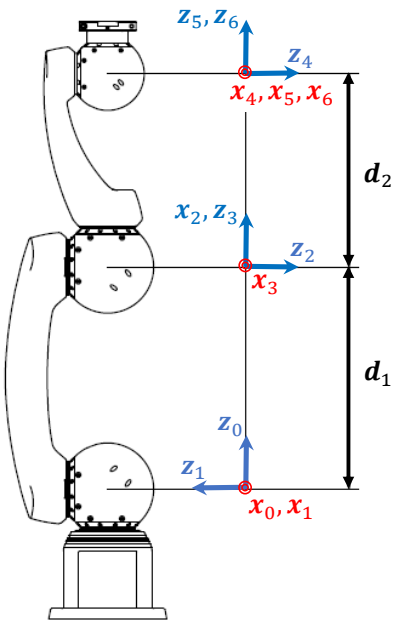

Figure 2. D-H Frames of the Powerball

Table 1. D-H Parameters

Link	a_i	α_i	d_i	θ_i
1	0	$\pi/2$	0	q_1
2	$0.350\ m$	π	0	$q_2 + \pi/2$
3	0	$\pi/2$	0	$q_3 + \pi/2$
4	0	$-\pi/2$	$0.305\ m$	q_4
5	0	$\pi/2$	0	q_5
6	0	0	0	q_6

The transformation matrix from Frame i to Frame $i-1$ can be calculated by

$$T_i^{i-1}(q_i) = \begin{bmatrix} Cq_i & -Sq_iC\alpha_i & Sq_iS\alpha_i & a_iCq_i \\ Sq_i & Cq_iC\alpha_i & -Cq_iS\alpha_i & a_iSq_i \\ 0 & S\alpha_i & C\alpha_i & d_i \\ 0 & 0 & 0 & 1 \end{bmatrix} \quad (1)$$

where the notations S and C denote cosine and sinus, respectively.

Therefore, the transformation describing the pose of the last frame with respect to frame 0 can be computed by

$$T_e^b(\mathbf{q}) = T_1^0(q_1)T_2^1(q_2)\dots T_6^5(q_6) = \begin{bmatrix} \mathrm{n}_e^b(\mathbf{q}) & \mathrm{s}_e^b(\mathbf{q}) & \mathrm{a}_e^b(\mathbf{q}) & \mathrm{p}_e^b(\mathbf{q}) \\ 0 & 0 & 0 & 1 \end{bmatrix} \quad (2)$$

where p_e^b is the position and n_e^b, s_e^b, a_e^b are the unit vectors of the last frame with respect to the base frame.

B. Dynamic Model

The equations of motion can be obtained utilizing the Lagrange formulation that is shown in Eqn. 3. In this equation Lagrangian of the system is defined by the robot kinetic energy minus its potential energy (Eqn. 4),

$$\frac{d}{dt}\left(\frac{\partial L}{\partial \dot{\mathbf{q}}}\right)^T - \left(\frac{\partial L}{\partial \mathbf{q}}\right)^T = \boldsymbol{\tau} \tag{3}$$

$$L = T - U = \sum_{i=1}^{6} (T_i - U_i) \tag{4}$$

where $\mathbf{q}$ and $\dot{\mathbf{q}}$ denote vectors of joint positions and velocities, respectively, and $\boldsymbol{\tau}$ is the vector of joint torques.

An important property of the robot manipulators, which is useful for the identification procedure, is linearity of the dynamic model with respect to the dynamic parameters [8]. By defining the augmented link i as a combination of both link i and rotor $(i+1)$, kinetic and potential energies of the augmented link i can be expressed in a linear form with respect to the dynamic parameters as shown in Eqn. 5 and 6,

$$\begin{aligned} T_i = {} & \frac{1}{2} m_i \dot{\boldsymbol{p}}_i^{iT} \dot{\boldsymbol{p}}_i^i + \dot{\boldsymbol{p}}_i^{iT} \boldsymbol{S}(\boldsymbol{\omega}_i^i) m_i \boldsymbol{r}_{i,C_i}^i + \frac{1}{2} \boldsymbol{\omega}_i^{iT} \hat{\boldsymbol{I}}_i^i \boldsymbol{\omega}_i^i \\ & + k_{r,i+1} \dot{q}_{i+1} I_{m_{i+1}} z_{m_{i+1}}^{iT} \boldsymbol{\omega}_i^i \\ & + \frac{1}{2} k_{r,i+1}^2 \dot{q}_{i+1}^2 I_{m_{i+1}} \end{aligned} \tag{5}$$

$$U_i = -\boldsymbol{g}_0^{iT} (m_i \boldsymbol{p}_i^i + m_i \boldsymbol{r}_{i,C_i}^i) \tag{6}$$

where,

m_i: total mass of augmented link i
$\dot{\boldsymbol{p}}_i^i$: linear velocity of augmented link i with respect to frame i
$\boldsymbol{\omega}_i^i$: angular velocity of augmented link i referred to frame i
$\boldsymbol{r}_{i,C_i}^i$: center of mass vector of augmented link i expressed in frame i, which is defined by $r_{i,C_i}^i = [\ell_{C_ix} \quad \ell_{C_iy} \quad \ell_{C_iz}]^T$
$k_{r,i+1}$: gear reduction ratio of actuator $(i+1)$
$I_{m_{i+1}}$: inertia of rotor $(i+1)$
$z_{m_{i+1}}^i$: unit vector along the rotor axis
$\boldsymbol{p}_i^i$: position vector of link i with respect to frame i
$\boldsymbol{g}_0^i$: gravity acceleration vector expressed in frame i
$\boldsymbol{S}(.)$: skew-symmetric matrix operator that transforms the components of the vector $r = [r_x \quad r_y \quad r_z]^T$ into the following form:

$$\boldsymbol{S}(r) = \begin{bmatrix} 0 & -r_z & r_y \\ r_z & 0 & -r_x \\ -r_y & r_x & 0 \end{bmatrix} \tag{7}$$

$\hat{\boldsymbol{I}}_i^i$: inertia tensor of augmented link i relative to its center of mass when expressed in the frame i,

$$\hat{\boldsymbol{I}}_i^i = \begin{bmatrix} \hat{I}_{ixx} & -\hat{I}_{ixy} & -\hat{I}_{ixz} \\ -\hat{I}_{ixy} & \hat{I}_{iyy} & -\hat{I}_{iyz} \\ -\hat{I}_{ixz} & -\hat{I}_{iyz} & \hat{I}_{izz} \end{bmatrix} \tag{8}$$

Using the above definition of kinetic and potential energies, the Lagrangian of the system can be rewritten in a linear form with respect to the (11×1) vector of the dynamic parameters, $\boldsymbol{\pi}$, including the mass (m_i), three components of the first-order momentum $(m_i \boldsymbol{r}_{i,C_i}^i)$, six components of the symmetric inertia matrix of the augmented link $(\hat{\boldsymbol{I}}_i^i)$ and moment of inertia of the rotor (I_{m_i}),

$$L = \sum_{i=1}^{6} (\beta_{T_i}^T - \beta_{U_i}^T)\, \boldsymbol{\pi}_i \tag{9}$$

$$\begin{aligned} \boldsymbol{\pi}_i = [\ & m_i \quad m_i \ell_{C_ix} \quad m_i \ell_{C_iy} \quad m_i \ell_{C_iz} \quad \hat{I}_{ixx} \\ & \hat{I}_{ixy} \quad \hat{I}_{ixz} \quad \hat{I}_{iyy} \quad \hat{I}_{iyz} \quad \hat{I}_{izz} \quad I_{m_i}\ ]^T \end{aligned} \tag{10}$$

where β_{U_i} is a (11×1) vector and is a function of the joint position q_i, while β_{T_i} is a (11×1) vector depending on the joint position q_i and its angular velocity $\dot{q}_i$. Taking derivative of the above Lagranigan does not affect its linearity with respect to defined dynamic parameters. Therefore, the equations of motion can be expressed in a linear form. They can be rewritten as,

$$\boldsymbol{\tau} = \boldsymbol{Y}(\mathrm{q}\,, \dot{\mathrm{q}}\,, \ddot{\mathrm{q}})\boldsymbol{\pi} \tag{11}$$

where $\boldsymbol{Y}$ is a (6×66) upper triangular matrix called "regressor" depending only on the robot kinematic parameters, and $\boldsymbol{\pi}$ is a (66×1) vector of all dynamic parameters of the robotic manipulator ($\boldsymbol{\pi} = [\boldsymbol{\pi}_1^T \boldsymbol{\pi}_2^T \ldots \boldsymbol{\pi}_6^T]^T$).

One of characteristics of Eqn. 11 is that in most cases not all the dynamic parameters affect the joint torques and this would result in rank deficient regressor. Thus, the dynamic parameters can be divided into three different groups [9][10]:

1) Unidentifiable parameters that correspond to zero column of the regressor.
2) Absolutely identifiable parameters which are related to linearly independent columns of the regressor
3) Identifiable parameters in linear combination with other parameters which correspond to linearly dependent columns of the regressor.

Therefore, the size of $\boldsymbol{\pi}$ can be reduced by eliminating unidentifiable parameters and combining linearly dependent identifiable parameters. The minimum set of parameters that are required for dynamic model is known as the base parameters. The length of base parameters is equal to the rank of regressor. Therefore, the vector of dynamic parameters $\boldsymbol{\pi}$ and the regressor $\boldsymbol{Y}$ in Eqn. 11 can be replaced by the base paramteres and reduced regressor, respectively.

Calculating the base parameters and reducing the regressor can be performed both analytically and numerically using QR decomposition and Singular Values Decomposition (SVD), respectively. Due to more precision, the SVD method has been utilized to reconstruct the base parameters and the corresponding regressor in this research.

More simplification of the base parameters is possible using the physical properties of the links and joints provided by the SCHUNK. By considering the mass distribution information and specific symmetries of the robot elements, the following parameters can be eliminated from the base parameters and its corresponding column of the regressor,

$$\begin{aligned}\ell_{C_1x} = \ell_{C_1z} = \ell_{C_2y} = \ell_{C_3x} = \ell_{C_4x} = \ell_{C_5x} = \ell_{C_6x} \\ = \ell_{C_6y} = \hat{I}_{1xy} = \hat{I}_{1xz} = \hat{I}_{1yz} = \hat{I}_{2xy} \\ = \hat{I}_{2yz} = \hat{I}_{3xy} = \hat{I}_{3xz} = \hat{I}_{4xy} = \hat{I}_{4xz} \\ = \hat{I}_{5xy} = \hat{I}_{5xz} = \hat{I}_{6xy} = \hat{I}_{6xz} = \hat{I}_{6yz} \\ = 0\end{aligned} \quad (12)$$

Considering simplified dynamic parameters of the augmented links and corresponding regressor, the SVD method has been used to extract the final base parameters for the Powerball and the result is given by,

$$\begin{aligned}\boldsymbol{\pi} = [\, & m_2\ell_{C_2x} \quad m_2\ell_{C_2z} \quad \hat{I}_{2xz} \quad m_3\ell_{C_3y} \quad m_3\ell_{C_3z} \\ & \hat{I}_{3yz} \quad I_{m_3} \quad m_4\ell_{C_4y} \quad m_4\ell_{C_4z} \quad \hat{I}_{4yz} \\ & I_{m_4} \quad m_5\ell_{C_5y} \quad m_5\ell_{C_5z} \quad \hat{I}_{5yz} \quad I_{m_5} \\ & m_6\ell_{C_6z} \quad \hat{I}_{R1} \quad m_{R1} \quad \hat{I}_{R2} \quad \hat{I}_{R3} \quad \hat{I}_{R4} \\ & \hat{I}_{R5} \quad m_{R2} \quad \hat{I}_{R6} \quad \hat{I}_{R7} \quad \hat{I}_{R8} \quad \hat{I}_{R9} \\ & \hat{I}_{R10} \quad \hat{I}_{R11}\,]^T\end{aligned} \quad (13)$$

Elements of the final base parameters show 29 dynamic parameters that are required to be identified for dynamic model of the Powerball. Subscript *R* denotes the regrouped parameters which are listed in Tab. 3. After identifying the base parameters, the Lagrangian of the system presented in Eqn. 9 can be calculated in terms of joint angles and velocities, and the equations of motion for the system can be rewritten in the following usual form,

$$\boldsymbol{B}(\mathbf{q})\ddot{\mathbf{q}} + \boldsymbol{C}(\mathbf{q},\dot{\mathbf{q}})\dot{\mathbf{q}} + \mathbf{g}(\mathbf{q}) + \boldsymbol{f} = \boldsymbol{\tau} \quad (14)$$

where $\boldsymbol{B}(\mathbf{q})$ denotes (6×6) symmetric positive definite matrix of robot inertia, $\boldsymbol{C}(\mathbf{q},\dot{\mathbf{q}})$ is the (6×6) matrix of Coriolis and centrifugal effects, $\mathbf{g}(\mathbf{q})$ is the (6×1) gravity vector, $\boldsymbol{\tau}$ represents the (6×1) motor torque vector, and $\boldsymbol{f}$ is the vector of friction torque that is discussed in the next section.

C. Friction Model

Precise positioning, zero backlash and compact size of the harmonic drives make them ideal for manipulator joints; however, one of their major drawbacks is their high levels of friction. The major part of this friction caused by their flex-spline.

For modeling friction a wide range of models has been proposed in the literature and most of them have been reviewed by Armstrong-H´elouvry et al. [11] and Olsson et al. [12]. Although in reality the behavior of friction in the robot joint is complicated, some studies utilized the following simple model of friction which is a combination of viscous and Coulomb frictions for the robot joints,

$$f_i = F_{ci}sign(\dot{q}_i) + F_{vi}\dot{q}_i \quad (15)$$

where F_{ci} and F_{vi} represent the Coulomb and viscous friction coefficients of joint i, respectively. By assuming friction torque as a linear function of joint position and velocity, i.e. given model in Eqn. 15, the friction coefficients can be considered as the base parameters; however, as it is observed for Powerball, this assumption cannot be verified by experimental data and results in considerable errors in the value of identified parameters.

In order to analyze the friction model, a large number of experiments have been conducted for each of the six joints. For this purpose the "velocity control mode" of the ERB modules has been used, because this mode of operation has the ability of accurate velocity tracking even at very low velocities. In this procedure, for each joint the manipulator was mounted in such configuration that the gravity has no effect on the joint torque. These configurations are achievable by mounting the robot base vertically or horizontally such that the joint axis lies along the gravity acceleration vector.

During the conducting experiments, dependency of the friction model to the time of experiment reveals that temperature has an important effect on the model of friction in Powerball joints. In fact, over the course of the experiments, the temperature of harmonic drive increased and results in change of lubricant state. In most of the studies the temperature is considered to be constant and the effect of temperature on the modeling of friction is ignored; however, in Powerball this assumption leads to significant degradation of the accuracy of the identified parameters.

In order to show the effect of temperature on the friction model, a sinusoidal trajectory is executed to the 4th joint of the robot periodically. The magnitude of the trajectory were chosen in such a way that the resultant motion avoids joint limits. Time and motor torque are recorded during the maneuver. For each cycle, the mean torque value of trajectory tracking during a complete period has been calculated. The experimental data points and exponential fitted model are illustrated in Fig. 3.

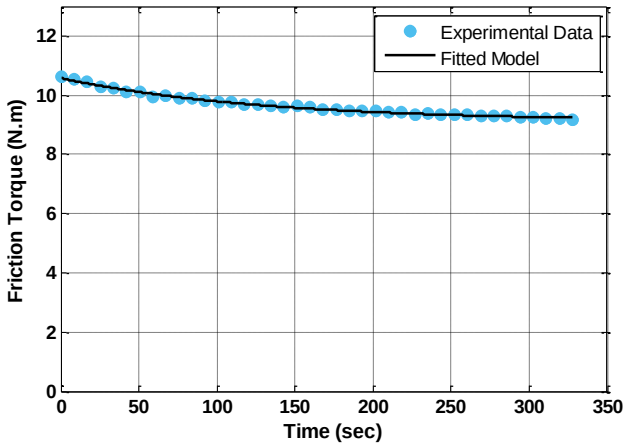

Figure 3. Change of friction over time

As it is shown in Fig. 3, for a periodic motion the value of mean torque decreases over time exponentially. This change is consistent with the lubricant character that the viscosity decreases over temperature increase and has been introduced in the studies of tribology [13]. Moreover, a difference of about ten percent between maximum and minimum values of mean torques in Fig. 3 demonstrates the importance of the temperature effect on the modeling of friction.

In order to minimize the effect of temperature on the friction torque of the robot joints, a systematic procedure

named "warm-up" has been developed. The warm-up process is used after powering the robot on and through this procedure each joint of the robot starts to move harmonically until the rate of change in mean torque of the consecutive cycles reaches a specific small value.

For mathematical modeling of friction at the robot joints, data for different velocities between 0.01 rad/s to 0.55 rad/s have been gathered from the robot controller interface. For each velocity, the mean value of the recorded joint torques has been calculated and used for mathematical fitting procedure. To check existence of Stribeck effect, for the velocities within the range of 0.01 to 0.2 rad/s the experimental data has been collected at 11 sampling points, while for the higher velocities within 0.2 to 0.55 rad/s only 7 sampling points are gathered. A same experiment is repeated for negative velocities as well to construct the friction curve. To eliminate the effect of gravity effect on the friction torques, data gathering for joints 1, 4, 5, and 6 have been performed in a vertical mounting of the robot base, while for joints 2 and 3 the robot base was mounted horizontally.

From the gathered data, the velocity dependent characteristic of friction was observed and all the robot joints have had the following characteristics:

- The Stribeck effect was not observed
- Viscous friction behaved linearly proportional to velocity at low velocities and its coefficient decreased at high velocities

Because discontinuous and piecewise continuous friction models are not suitable for implementation of a high performance continuous controller, a continuously differentiable friction model as the combination of hyperbolic terms has been used to model friction at each joint. The original hyperbolic friction model proposed by Makkar et al. [14], consists of six parameters to capture the Stribeck and velocity dependent frictional characteristics. But since the Stribeck effect was not observed in the Powerball joints, the hyperbolic model is modified to the following five parameter model,

$$f_i = \gamma_{1i}\tanh(\gamma_{2i}\dot{q}_i) + \gamma_{3i}\tanh(\gamma_{4i}\dot{q}_i) + \gamma_{5i}\dot{q}_i \qquad (16)$$

where $\gamma_k, k = 1,..,5$ are the model parameters. Experimental data along with the fitted models are illustrated in Fig. 4 to 6. Nonlinear Least Squares techniques are utilized to fit overdetermined data set to the proposed model. Estimated values of the five design variables of friction models are listed in Tab. 2.

Table 2. Estimated parameter values of the friction model

Joint	γ_1	γ_2	γ_3	γ_4	γ_5
1	4.58	215.56	2.11	4.70	14.76
2	4.73	216.73	2.89	5.11	17.04
3	4.59	224.53	2.42	4.95	15.94
4	4.51	200.66	1.91	3.33	12.14
5	0.05	11.36	0.28	793.63	0.41
6	0.05	10.59	0.27	782.43	0.37

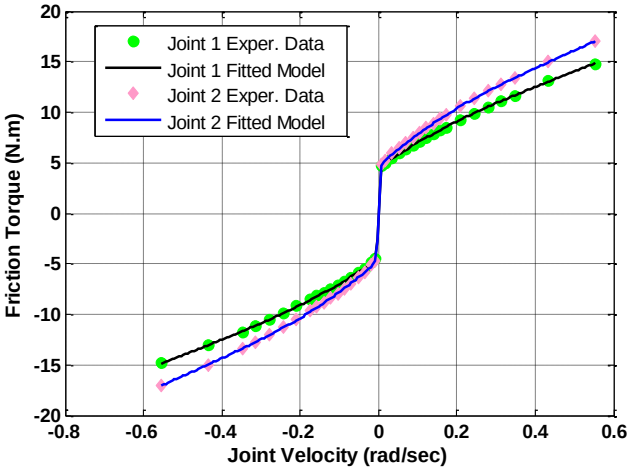

Figure 4. Friction experimental data and fitted model for joints 1 and 2

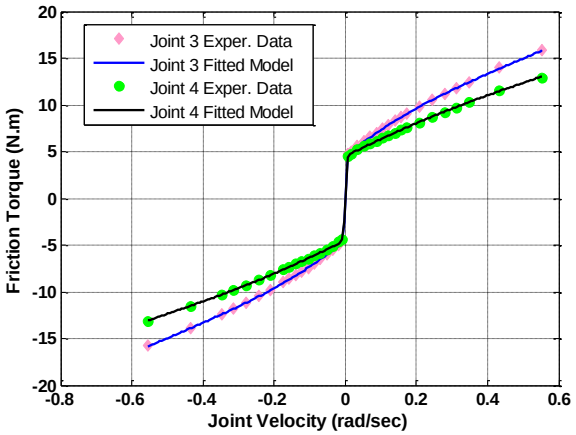

Figure 5. Friction experimental data and fitted model for joints 3 and 4

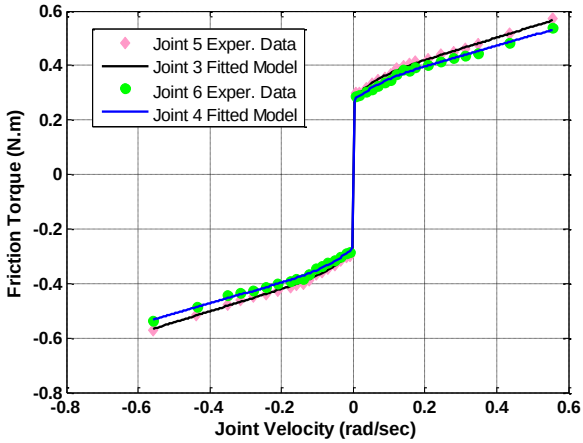

Figure 6. Friction experimental data and fitted model for joints 5 and 6

III. EXPERIMENTAL RESULTS

A. Experimental Setup

The experimental setup consisted of the SCHUNK Powerball LWA 4P, a 24v DC power supply and a PC running GNU/Linux operation system. The Powerball communication protocol is based on CANopen (CiA DS402 standard protocol) and only one CAN bus interface is enough for controlling all the axes. In this setup, a high-speed USB to CANopen adaptor has been used to establish communication between the operation system and ERB modules.

In order to communicate with CANopen servo drivers embedded at each joint and control the motion of robotic arm, a C++ library has been developed. Currently, the library provides an Application Programming Interface (API) including the necessary functions to control the robot joints in current, velocity and interpolated position modes. The controller runs at a sampling rate of 200 Hz. During each sampling interval the PC receives the axes states including measured motor position, velocity and current, and also provides each servo controller with the reference set point. In addition, motor positions are measured by shaft incremental encoders mounted on the motor sides and electro-magnetic brakes are used for inactivating robot links.

B. Exciting Trajectory

The numerical efficiency of identifying the dynamic parameters can be improved by a well-designed trajectory that excites the dynamical properties of the robot links during motion. In order to achieve such trajectory, a multi-objective optimization problem should be solved. The criteria of the optimization problem is minimizing the condition number and maximizing minimum singular value of the regressor matrix along the trajectory. Therefore, a small sensitivity to the measurement noise and model uncertainties will be guaranteed during estimation of the dynamic parameters using Least Square techniques. For this purpose, the nonlinear optimization criteria can be expressed as,

$$\begin{aligned} &Minimize\ G(\mathrm{q}\,,\dot{\mathrm{q}}\,,\ddot{\mathrm{q}}) \\ &s.t\begin{cases}|\mathrm{q}| < \mathrm{q}_{\mathrm{Lim}} \\ |\dot{\mathrm{q}}| < \dot{\mathrm{q}}_{\mathrm{Lim}} \\ |\ddot{\mathrm{q}}| < \ddot{\mathrm{q}}_{\mathrm{Lim}}\end{cases} \\ &where, \quad G(\mathrm{q}\,,\dot{\mathrm{q}}\,,\ddot{\mathrm{q}}) = \lambda_1 \mathrm{cond}(\boldsymbol{Y}) + \lambda_2 \frac{1}{\sigma_p(\boldsymbol{Y})} \end{aligned} \tag{17}$$

where $\mathrm{cond}(\boldsymbol{Y})$ and $\sigma_p(\boldsymbol{Y})$ represent the condition number and smallest singular value of the regressor matrix, respectively; hence λ_1 and λ_2 denote their weighting coefficients. The position, velocity and acceleration constraints are provided by the manufacturer and prevent the joints reach their limit and protect them from overload. The finite Fourier series has been chosen as the base function for approximating optimal exciting trajectory. Using the finite Fourier series improves the computational robustness and reliability by providing smooth velocity and acceleration profiles. Thus, the angular position, velocity and acceleration for the joints are given by,

$$q_i(t) = \sum_{l=1}^{N_i} \frac{a_l^i}{\omega_f l}\sin(\omega_f lt) - \frac{b_l^i}{\omega_f l}\cos(\omega_f lt) + q_{i0} \tag{18}$$

$$\dot{q}_i(t) = \sum_{l=1}^{N_i} a_l^i \cos(\omega_f lt) + b_l^i \sin(\omega_f lt) \tag{19}$$

$$\ddot{q}_i(t) = \sum_{l=1}^{N_i} -a_l^i \omega_f l \sin(\omega_f lt) + b_l^i \omega_f l \cos(\omega_f lt) \tag{20}$$

where ω_f denotes the fundamental frequency of Fourier serious. a_l^i and b_l^i are the amplitudes of harmonics which are the design variables of the optimization problem given in Eqn. 17. Figure 8 shows the designed exciting trajectories for a fundamental frequency of $\omega_f = 2\pi/10$ and $N = 4$.

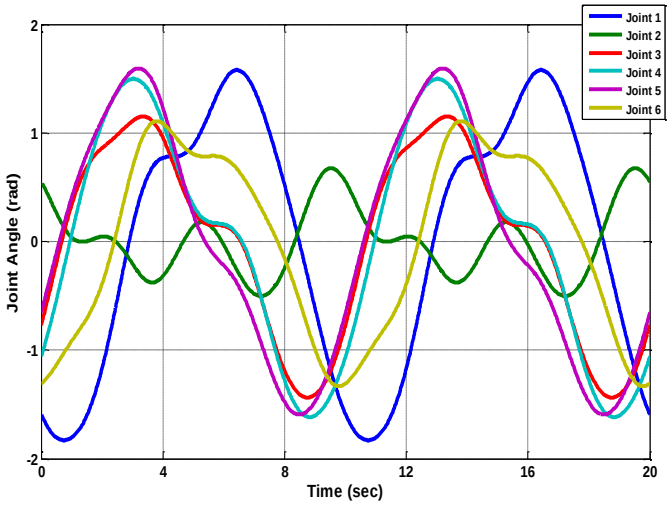

Figure 7. Designed exciting trajectories

C. Dynamic Parameter Identification

Designed exciting trajectory profiles have been executed to the robot joints for the purpose of dynamic parameter identification. In order to track desired trajectories, mode of operation of the ERB modules were set to "interpolated position mode". Although uncorrelated input and output signals requires an open-loop data, it was not feasible due to the safety reasons. Motor positions, velocities and currents have been recorded at a sampling rate of 200 Hz.

During the experiment, the joint angles were measured by means of motor shaft encoders with a resolution of 0.001 degree. Motor torques have been computed by converting motor currents into the torque values using provided torque constants by manufacturer. A decimation filter has been applied on the measured torques, while accelerations of the joints are numerically estimated off-line from the measured velocities and utilizing a Butterworth bandpass filter. Computed values of dynamic parameters for the Powerball are listed in Tab. 3.

Table 3. Identified values of Powerball dynamic parameters

Parameter	Value	Parameter	Value
$m_2\ell_{C_{2x}}$	$-3.45e^{-2}$	$m_6\ell_{C_{6z}}$	$2.37e^{-1}$
$m_2\ell_{C_{2z}}$	1.53	$\hat{I}_{1yy}+\hat{I}_{2yy}+\hat{I}_{3zz}+I_{m_1}$	-2.01
$\hat{I}_{2xz}$	$-2.6e^{-1}$	m_2+m_3	2.05
$m_3\ell_{C_{3y}}$	$-1.94e^{-1}$	$\hat{I}_{2xx}-\hat{I}_{2yy}$	3.78
$m_3\ell_{C_{3z}}$	$-1.33e^{-1}$	$\hat{I}_{2zz}+I_{m_2}$	$-8.35e^{-1}$
$\hat{I}_{3yz}$	$-9.15e^{-2}$	$\hat{I}_{3xx}-\hat{I}_{3zz}+\hat{I}_{4zz}$	-1.03
I_{m_3}	$8.31e^{-2}$	$\hat{I}_{3yy}+\hat{I}_{4zz}$	$1.72e^{-1}$
$m_4\ell_{C_{4y}}$	$4.75e^{-1}$	$m_4+m_5+m_6$	4.5
$m_4\ell_{C_{4z}}$	$8.99e^{-2}$	$\hat{I}_{4xx}-\hat{I}_{4zz}+\hat{I}_{5zz}-I_{m_6}$	$-2.3e^{-1}$
$\hat{I}_{4yz}$	$-4.08e^{-2}$	$\hat{I}_{4yy}+\hat{I}_{5zz}-I_{m_6}$	$8.44e^{-2}$
I_{m_4}	$4.94e^{-1}$	$\hat{I}_{5xx}+\hat{I}_{6yy}-\hat{I}_{5zz}+I_{m_6}$	$1.25e^{-2}$
$m_5\ell_{C_{5y}}$	$-1.46e^{-1}$	$\hat{I}_{5yy}+\hat{I}_{6yy}$	$-1.69e^{-1}$
$m_5\ell_{C_{5z}}$	$-2.64e^{-1}$	$\hat{I}_{6xx}-\hat{I}_{6yy}$	$5.28e^{-2}$
$\hat{I}_{5yz}$	$2.04e^{-2}$	$\hat{I}_{6zz}+I_{m_6}$	$-3.17e^{-2}$
I_{m_5}	$1.64e^{-1}$		

D. Experimental Verification

Validity of the extracted dynamic parameters for the Powerball are verified by executing a second sinusoidal trajectory covering most of the robot work space. For this trajectory, the joint torques are estimated by substituting the recorded experimental data including joint positions, velocities and accelerations into the robot inverse dynamics model (Eqn. 11). Estimated joint torques are compared to measured torque values and the errors between them are calculated during the robot maneuver. Figure 8 shows the measured and reconstructed motor torques for all the six axes using identified base parameters. Small estimation errors demonstrate the accuracy of the estimated dynamic parameters for the Powerball robotic arm.

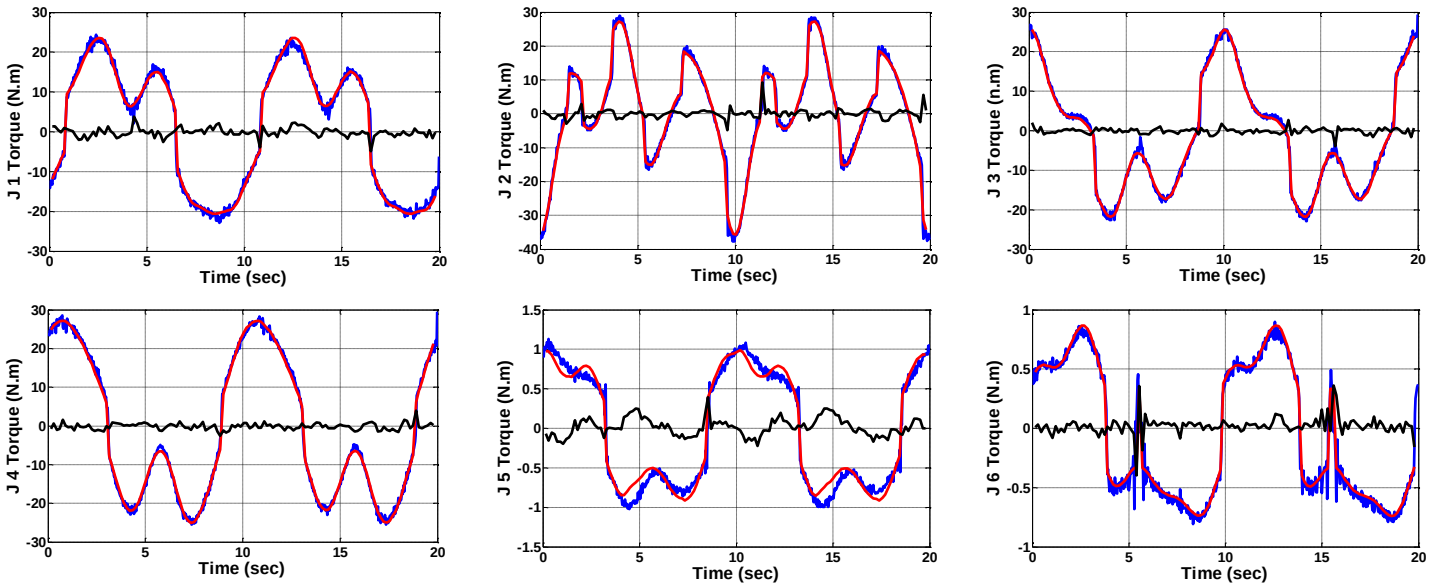

Figure 8. Measured (blue) and estimated (red) joint torque with error (black) during verification experiment

IV. CONCLUSION

In this paper, modeling and identification of the SCHUNK Powerball robotic arm was performed. The dynamic parameters of the robot have been reconstructed into a simplified identifiable form. The friction behavior of the joints has been investigated experimentally and based on the results a nonlinear model was proposed for estimating friction at each joint. An optimal exciting trajectory was designed in order to perform identification process. The Powerball dynamic parameters have been estimated utilizing Least Square techniques. The correctness of the identified dynamic model was validated by reconstructing torques using the identified model along a verification trajectory and comparing them to measured torques.

REFERENCES

[1] W. Khalil, E. Dombre, and M. Nagurka, "Modeling, Identification and Control of Robots," *Applied Mechanics Reviews*, vol. 56. p. B37, 2003.

[2] J. Hollerbach, W. Khalil, and M. Gautier, "Model Identification," in *Springer Handbook of Robotics*, Springer, 2008.

[3] M. Gautier and W. Khalil, "Direct calculation of minimum set of inertial parameters of serial robots," *IEEE Trans. Robot. Autom.*, vol. 6, pp. 368–373, 1990.

[4] N. A. Bompos, P. K. Artemiadis, A. S. Oikonomopoulos, and K. J. Kyriakopoulos, "Modeling, full identification and control of the mitsubishi PA-10 robot arm," in *IEEE/ASME International Conference on Advanced Intelligent Mechatronics, AIM*, 2007.

[5] C. Gaz, F. Flacco, and A. De Luca, "Identifying the dynamic model used by the KUKA LWR: A reverse engineering approach," in *Robotics and Automation (ICRA), 2014 IEEE International Conference on*, 2014, pp. 1386–1392.

[6] A. Jubien, M. Gautier, and A. Janot, "Dynamic identification of the Kuka LightWeight robot: Comparison between actual and confidential Kuka's parameters," in *Advanced Intelligent Mechatronics (AIM), 2014 IEEE/ASME International Conference on*, 2014, pp. 483–488.

[7] M. Gautier and W. Khalil, "Exciting trajectories for the identification of base inertial parameters of robots," *[1991] Proc. 30th IEEE Conf. Decis. Control*, 1991.

[8] B. Siciliano, L. Sciavicco, L. Villani, and G. Oriolo, *Robotics: Modelling, Planning and Control*. 2009, p. 632.

[9] F. Caccavale and P. Chiacchio, "Experiments of feedforward control on a conventional industrial manipulator," *Proc. 1994 Am. Control Conf. - ACC '94*, vol. 1, 1994.

[10] G. Antonelli, F. Caccavale, and P. Chiacchio, "A systematic procedure for the identification of dynamic parameters of robot manipulators," *Robotica*, vol. 17. pp. 427–435, 1999.

[11] B. Armstrong-Hélouvry, P. Dupont, and C. C. De Wit, "A survey of models, analysis tools and compensation methods for the control of machines with friction," *Automatica*, vol. 30. pp. 1083–1138, 1994.

[12] H. Olsson, K. K. J. Åström, C. Canudas de Wit, M. Gäfvert, and P. Lischinsky, "Friction Models and Friction Compensation," *Eur. J. Control*, vol. 4, pp. 176–195, 1998.

[13] B. Bhushan, *Modern Tribology Handbook, Two Volume Set*. 2000, p. 1760.

[14] C. Makkar, W. E. Dixon, W. G. Sawyer, and G. Hu, "A new continuously differentiable friction model for control systems design," *Proceedings, 2005 IEEE/ASME Int. Conf. Adv. Intell. Mechatronics.*, 2005.